Tellus (2006), 58A, 584–592
Printed in Singapore. All rights reserved

TELLUS

Winter time flow over and around Greenland: trajectories related to torques

By JOSEPH EGGER*, *Meteorologisches Institut der Universität München, Theresienstrasse 37, 80333 München, Germany*

(Manuscript received 26 January 2006; in final form 2 June 2006)

ABSTRACT

Results of first steps towards a dynamically oriented climatology of winter time flow over and around Greenland are presented. The synoptic situations in the Greenland area are classified with respect to Greenland's axial mountain torque. This torque is positive (negative) if the surface pressure at the eastern slope is higher (lower) than at the windward side. Mean trajectories are calculated from correlations of observed flows with the torque. Three classes of trajectories are formed: 'blocked', 'over' and 'around'. It is found for low-level starting points west of Greenland, that blocked trajectories are most common for positive torques while the bulk of the trajectories is deflected around Greenland or crosses the massif for negative torques. These results are shown to be broadly consistent with the standard non-dimensional height criterion. Flow splitting is common to the west of Greenland. Stagnation points are found west of Greenland but also above the eastern slopes. Tip jets occur for negative torque events only.

1. Introduction

Greenland with its pronounced meridional orientation and relatively smooth shape provides a testbed for theories of air flow over and around large-scale mountains. For example, Petersen et al. (2003) studied the flow over an idealized Greenland topography of height h as a function of non-dimensional mountain height $\hat{h} = Nh/U$ and compared their results to realistic flow situations. They found that non-dimensional heights $\hat{h} \geq 3$ are necessary for upstream blocking to occur. The sea level pressure deficit in the lee grows with $\hat{h}$. The crossing of Greenland by cyclones from the west has been investigated numerically by Egger (1972) who found a splitting of the cyclones at the western wall and some kind of cyclogenesis in the lee when the low's upper part arrives above the lee slopes. Schwierz (2001) calculated the stationary response of Greenland to impinging barotropic westerly flow. A strong anticyclone forms above Greenland and a trough in the lee. Vortices are steered anticyclonically around Greenland in this quasistationary flow. Schwierz and Davies (2003) presented an example of cyclone motion near Greenland which illustrates these calculations. The formation of jets near the southern tip of Greenland (e.g. Moore and Renfrew, 2005) has been simulated and discussed by Doyle and Shapiro (1999). Wave breaking events as observed over Greenland have been simulated and compared to theoretical work by Doyle et al. (2005). In this case, good data coverage was provided by a field campaign. In general, however, there appears to be a certain gap between theoretical work and observations because the calculations tend to assume rather simple situations. For example, numerical investigations of upstream blocking, flow splitting and wake formation (e.g. Schär and Smith, 1993; Smith and Grønås, 1993; Schwierz, 2001; Petersen et al., 2003) tend to assume stationary inflow. Although the numerical simulations do not always reach steady state (e.g. Ólafsson and Bougeault, 1996; Petersen et al., 2003), at least the upstream transience is small compared to the situation near Greenland, where the inflow exhibits a complicated structure in space and time. In particular, synoptic perturbations are crossing Greenland or passing to the south so that undisturbed flow towards Greenland is the exception and not the rule. To bridge this gap, an observational basis must be established for intercomparison with the theoretical results obtained so far. Which part of the inflow will make it to climb over Greenland, which part is deflected around. Is there blocking of the flow? Do stagnation points exist? The answers to such questions depend, of course, on the synoptic situation. Although Walden (1959; see also Putnins, 1970) performed an extensive classification of cyclone paths near and over Greenland, his data base would not have allowed him to address such questions. Quite recently, Hoskins and Hodges (2002) published a detailed dynamic climatology of northern hemisphere stormtracks with particular emphasis on cyclone and anticyclone activity. However, features like flow splitting are not part of their analysis.

*Correspondence.
e-mail: J.Egger@lrz.uni-muenchen.de
DOI: 10.1111/j.1600-0870.2006.00198.x

It has been demonstrated by Iskenderian and Salstein (1998), Weickmann (2003), Egger and Hoinka (2006; EH) and others that the axial mountain torque is a convenient parameter for the classification of synoptic situations. Normally, the axial mountain torque is evaluated in order to determine the transfer of angular momentum with respect to the earth's rotation axis from the earth to the atmosphere at the mountain. The related drag affects the zonal flow and is, therefore, of dynamical interest. Positive torques imply a gain of atmospheric angular momentum. Here, these transfer aspects of the torque are of minor concern. Instead, we are interested in the flow situations related to torques because these situations capture much of the synoptic variability near a mountain. The axial mountain torque exerted by Greenland is

$$P = -\int_F p_s \frac{\partial h}{\partial \lambda} \mathrm{d}F. \qquad (1)$$

In (1), p_s is surface pressure, h is the topography of Greenland, λ is longitude and F is an area covering Greenland. The torque is obviously positive if the surface pressure at the eastern 'lee' slope is larger than at the western slope. Events with large torques (i.e. 'torque events') reflect the passage of synoptic systems near and over Greenland. In particular, low pressure systems move from the west toward the southeast near Greenland's tip during events with $P > 0$, while a ridge is built up above and to the east of Greenland (see also Fig. 2 and related comments below). Thus, the torque is growing during that time to decrease when the low in the south moves away over the lee-side high becomes weaker. Vice versa, lows prevail in the lee for $P < 0$. Hence, the torque P is a good indicator for synoptic situations near Greenland. Typical torque events have a duration of a few days only. Correspondingly, the autocorrelation of Greenland's mountain torque decays fairly quickly (EH). Of course, the torques changes little if, for example, storms move eastward south of Greenland. Such events are automatically excluded from our analysis. Torques are involved, however, whenever the atmosphere interacts with Greenland. Here, we are interested in such events.

EH correlated the flow fields as observed near Greenland with the torque P, so that we have flow fields as typical of torque events at our disposal. These statistical flows are now used to calculate trajectories. Given a certain value of P, we are able to find which part of the air flow goes around Greenland and which part climbs over the massif. This strategy invites, of course, the question why this statistical detour is made instead of calculating trajectories directly from the observed wind fields. There is, however, the problem that realistic trajectories cannot be stratified statistically with respect to a parameter (compromises will be discussed in Section 4). Instead, a novel method is proposed here which provides such stratified trajectories. Flow splitting, eventual crossing of the barrier and other features of dynamic interest can be investigated on the basis of statistical trajectories.

2. Data and strategy

The data to be used are part of the ERA 40 set covering the period January 1958–December 2001 generated by the European Center for Medium-Range Weather Forecast Reanalysis Project (Uppala et al., 2000). The trajectory analysis is restricted to the domain 81°W–0°W, 49.5°N–81°N selected by EH. In EH, wind, pressure and potential temperature data are transformed such that they are available at the original 1.125° × 1.125° horizontal grid and at 13 constant height surfaces with a vertical spacing Dz = 1000 m and the lowest surface at $z = 500$ m. Only winter seasons (DJF) will be considered. The winter mean torque is $\bar{P} = 2.2 \times 10^{18}$ J = 2.2 Hadley. All fields are available once a day as are the torques. To simplify the interpretation of results, the torque is normalized by its standard deviation of ~7 Hadley (see EH for details, 2006).

The flow statistics evaluated by EH consist mainly of covariances of the torque and grid point values of pertinent variables. Let $C(b, c|\tau)$ denote the covariance of a variable b with another variable c where b leads c with lag τ. All covariances $C(P, \mathbf{v}|\tau)$ of the torque $P(t)$ with the components of the velocity vector $\mathbf{v}$ $(x, y, z, t + \tau)$ are available and will be used to calculate trajectories. The lags are restricted to the interval $|\tau| \leq 5$ d because torque events are shortlived and covariances are small for $|\tau| >$ 5. The time mean flow $\bar{\mathbf{v}}(x, y, z)$ is available as well. Note, that the covariances are based on the data from all winter days contained in the ERA40 set.

Given a starting point $\mathbf{x}_0 = (x_0, y_0, z_0)$ at lag τ_0, we calculate a trajectory with respect to a given value P_0 of P by integrating

$$\frac{\mathrm{d}\mathbf{x}}{\mathrm{d}\tau} = C(P, \mathbf{v}(\mathbf{x})\,|\tau)P_0 + \bar{\mathbf{v}}(\mathbf{x}) \qquad (2)$$

with lag τ and $\mathbf{x}(\tau_0) = \mathbf{x}_0$. The resulting trajectory is the most likely one passing through $\mathbf{x}_o$ at $\tau = \tau_0$ for a torque P_0 at $\tau = 0$. There is no guarantee that this trajectory has ever been observed but it is typical in the sense that the winds used in the calculation are the mean winds with respect to all observations at lag τ given the value P_0 at $\tau = 0$. This wind field will provide the basic information on the flow over and around Greenland during torque events. The climatological mean flow is represented in (2) by the case $P_0 = 0$.

At this point, a caveat may be in order. Assume that the chosen parameter P is hardly correlated at all with the winds near Greenland. In that case, the first term on the right hand side of (2) is quite small. The trajectories follow essentially the mean flow. If, on the other hand, trajectories for, say, $P_0 = 2$ differ strongly from those for $P_o = -2$, this indicates that P is a relevant parameter. As will be seen, the mountain torque P is a suitable parameter.

In principle, (2) contains an infinitely large number of trajectories. In the following, the analysis is mainly restricted to the choices $P_0 = 0$, $P_0 = \pm 2$, that is, we look at the climatological mean flow and cases where torques amount to two standard deviations. A simple calculation shows that if the normalized

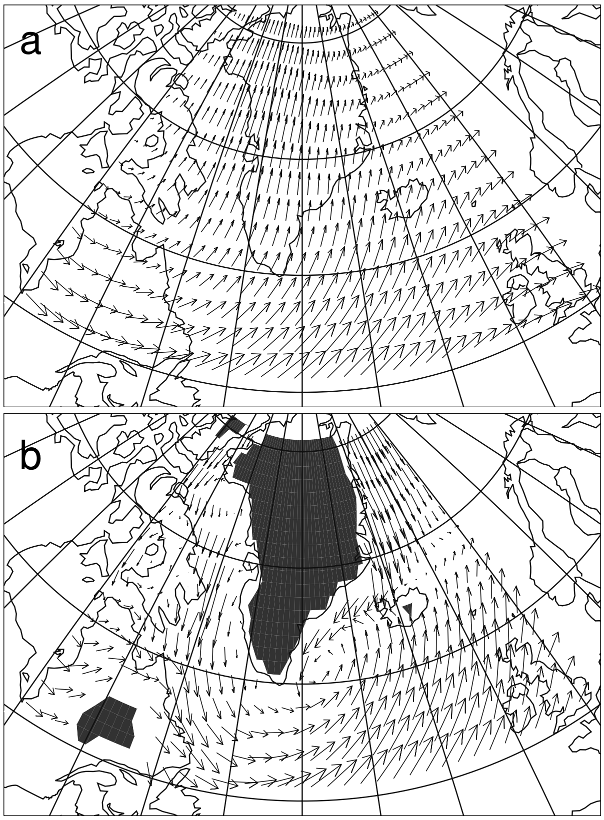

Fig. 1. Mean horizontal winds at levels $z = 5500$ m (a; maximum flow velocity 20.4 ms^{-1}) and $z = 500$ m (b; maximum flow velocity 8.0 m s^{-1}; dark: topography with heights > 500 m). Adapted from EH.

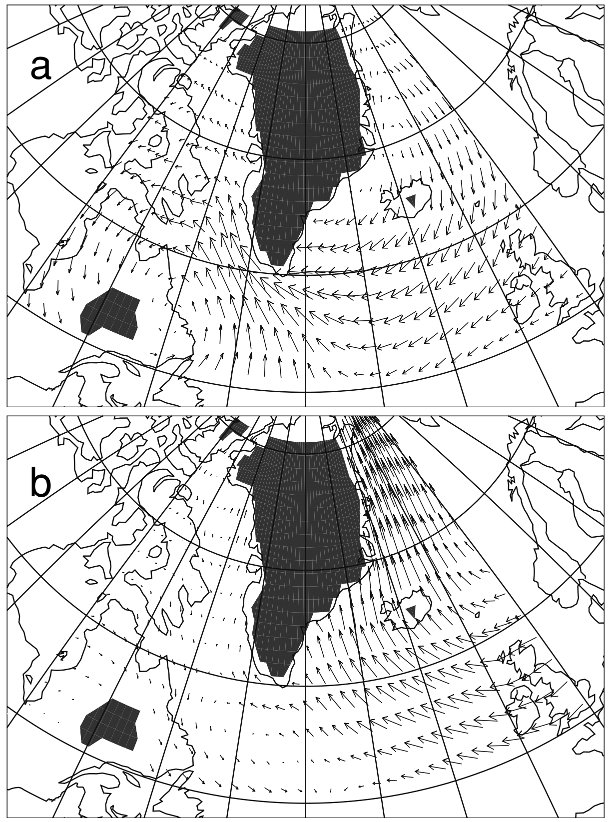

Fig. 2. Cross-covariance $C(P, \mathbf{v}|\tau)$ of the normalized Greenland mountain torque P with the horizontal wind at the level $z = 500$ m; (a) $\tau = -1$ d; maximum velocity 7.2 m s^{-1}; (b) $\tau = 2$ d; maximum velocity 3.2 m s^{-1}. Dark: topography with heights > 500 m. Adapted from EH.

torque $P_0 = 2$ is exerted for a day, the zonal mean wind field in the analysis domain would increase by 4 m s^{-1}. Thus, this torque implies a substantial acceleration. We have to keep in mind, however, that the zonal wind may even decrease during a toque event because of possible exports from the Greenland domain (see EH). Moreover, the mass distribution may play a role as well. As a matter of fact, EH demonstrated that the zonal mean momentum in the analysis domain decreases during events with positive torque.

The wind covariances as well as the mean winds in (2) vary smoothly in space and time (see also Figs. 1 and 2) so that relatively simple interpolation schemes can be used to evaluate the winds at the point **x**. We use quadratic interpolation in the horizontal and a linear one in the vertical. Interpolation in time is also linear. The trajectory equations (2) are solved with a forward time step $\mathrm{D}\tau = 30$ min. Intercomparisons with runs with somewhat longer time steps showed little sensitivity while a reduction to $\mathrm{D}\tau = 15$ min. left the results unaltered. Nevertheless, there is, of course, a slight dependence of the results on the numerical scheme used. On the other hand, the qualitative flow features to be discussed here appear not to depend significantly on the numerical details.

The mean wind field shows cyclonic flow around Greenland at the lowest level with northerlies in the west, westerlies south of Greenland and southerlies to south-westerlies in the east (Fig. 1; see also EH and Moore and Renfrew, 2005). The circulation of the Icelandic low is clearly visible. Note also the northerlies off the eastern slope of Greenland and the zone of confluence in the Norwegian sea. Higher up Greenland is embedded in the cyclonic southeasterly flow east of the planetary-scale stationary trough over Canada.

To provide an example for the flow evolution with changing torque, we show in Fig. 2 the cross-covariance $C(P, \mathbf{v}_2|\tau)$ of P with the horizontal wind at $z = 500$ m for $\tau = -1$ and 2 d. An event with $P > 0$ is accompagnied by an anticyclone east of Greenland and cyclonic flow in the west. The cyclone is located above Canada at $\tau = -1$ d and the high is situated above the eastern slope of Greenland. The low moves towards the southeast with increasing lag and has left the domain at $\tau = 2$ d. The anticyclone's center is also outside the analysis domain at that time so that southerlies prevail in the east. Of course, signs and flow directions have to be turned around for $P < 0$. Note,

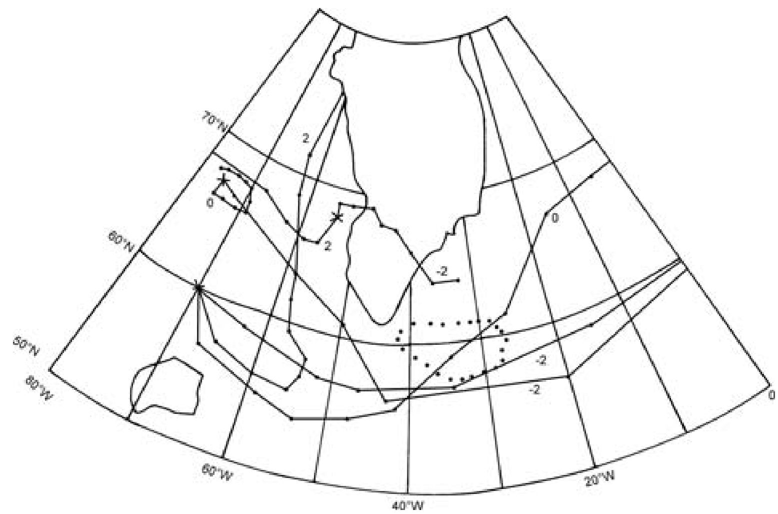

Fig. 3. Selected trajectories started at $\tau = -5$ d at the points marked by crosses. The number attached to a trajectory gives the value of the torque P at $\tau = 0$ for which this trajectory is calculated. Trajectory locations after a full day are indicated by a dot. The dots are connected by straight lines. The bold lines mark the border of Greenland and Canadian orography above $z = 500$ m. The dotted line encircles the area where zonal windspeeds > 13 m s^{-1} are found at $\tau = 0$ for $P = -2$ (tip jets).

that the winds displayed in Fig. 2 correspond with the first term on the right of (2) with $P_0 = 1$.

3. Results

3.1. Typical trajectories

To give the reader a feeling for the trajectories resulting from our analysis we present first a few examples for three starting points (Fig. 3). All trajectories start at $\tau = -5$ d at the lowest level and three calculations are carried out per starting point, one for $P = 0$, that is, for the climatological mean flow, one for $P = 2$ and one for $P = -2$. The trajectories for $P = 0$ and -2 simply pass Greenland in the westwind drift for the starting point at 70°W, 60°N. The trajectory for $P = 2$ is caught in the southerlies in between the low to the west of Greenland and the pronounced high above the eastern slope observed near $\tau = 0$ for $P > 0$ (see Fig. 2a). This particle moves to the north. A trajectory across Greenland is obtained for $P = -2$ for a start at 55°W, 67°N. On the other hand, the trajectory for $P = 2$ is mainly directed westward. That for $P = 0$ is similar but is not given to avoid confusion. The third starting point is located in the climatologically stagnating region at 75°W, 67°N (see Fig. 1). The trajectory for $P = 0$ stays in the region, that for $P = 2$ leaves the area in the west (not shown), while that for $P = -2$ goes around Greenland. Fig. 3 demonstrates clearly that variations of the torque have a profound impact on the trajectories.

3.2. Air flow over and around Greenland

In most trajectory calculations we start at $\tau_0 = -5$ d at all grid points west of Greenland. Trajectories are evaluated throughout the 10 d and the index m counts those moments when the trajectory is located above topography. Trajectories are said to go around Greenland if $m = 0$ and if the final position is to the east of the obstacle. They are said to be blocked if the final position is to the west of Greenland. Some of these trajectories stay for a while above Greenland so that $m \neq 0$, but the end point is located west of the Greenland massif. Trajectories over the mountain have $m \neq 0$ and the final point must be located above or to the east of Greenland. These are termed 'over'.

Let us first have a look at the climatological mean situation ($P = 0$). If the trajectories start at the lowest level ($z = 500$ m), some grid points must be excluded as starting points because they are located below the terrain height (see Fig. 3). There exist essentially three zonally oriented domains (Fig. 4a). Trajectories starting north of ~65°N are blocked, those with 60°N $\leq \tau \leq$ 65°N make it over the mountain and those further south tend to go around Greenland. The same analysis for starting points at $z =$ 1500 m yields an extension of the domain of crossing trajectories, while starting points of blocked trajectories are found only west of 57°W (Fig. 4b). It makes, of course, good sense to find more crossing trajectories and less blocked ones if the height of the departure points is increased.

For $P = -2$, there is high pressure to the west of Greenland and a low in the lee so that the anomalous winds are northerly above Greenland. This configuration wipes the blocked cases almost out. Crossing of the barrier occurs for low-starting trajectories close to Greenland while most trajectories go around the massif (Fig. 5a). Starts at $z = 1500$ m are followed most of the time by passages over Greenland and there are less trajectories leading around the obstacle (Fig. 5b). If, on the other hand, $P = 2$, blocking becomes dominant and trajectories have to start rather close to Greenland even at $z = 1500$ m to make it over the mountain (Figs. 6a and b).

No dramatic changes occur if the trajectories are started at $\tau = -3$ d. Of course, there are slight variations but the main features of Figs. 5 and 6 remain.

Altogether we find, that flow blocking is the dominant mode for $P = 2$ where an anticyclone is located near the east coast

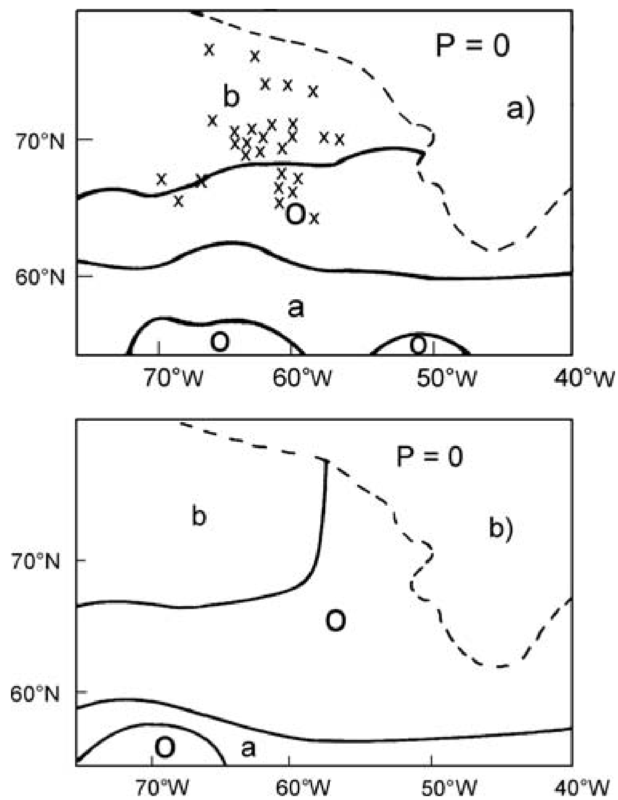

Fig. 4. Area where trajectories are started in a (λ, ϕ)-grid. The domains of blocked (b) trajectories, of those over Greenland (o) and of those around (a) are separated by bold lines. Greenland is indicated by the dashed line. Mountain torque $P = 0$. Starting height (a) 500 m, (b) 1500 m. The crosses mark the locations where flow splitting begins. See text for further details.

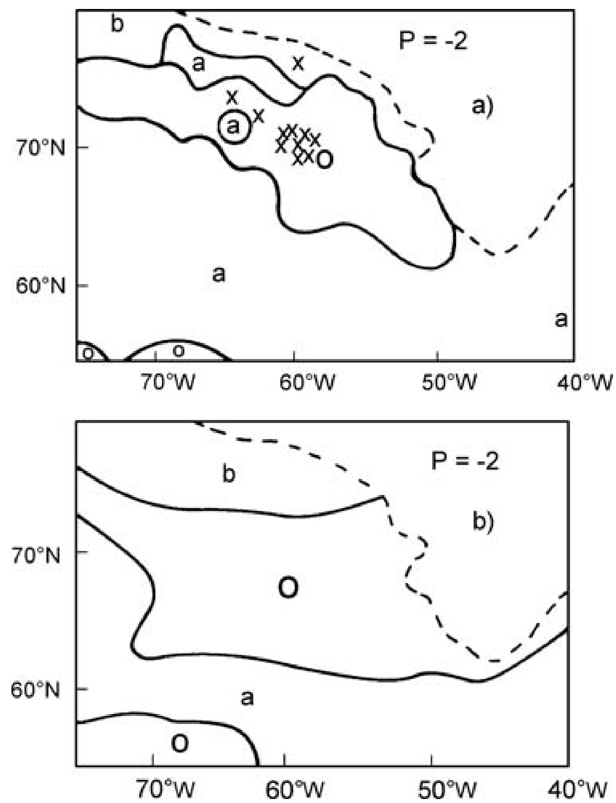

Fig. 5. As Fig. 4 but for $P = -2$.

of Greenland. On the other hand, most of the trajectories cross Greenland for $P = -2$ when there is a cyclone in the lee. That makes good sense because westerlies are anomalously strong above the southern part of Greenland in that case. Note also the similarity of Figs. 4b and 5b.

3.3. *Nondimensional mountain height*

As stated above, the nondimensional mountain height $\hat{h} = hN/U$ (N Brunt–Väisälä frequency; U mean zonal inflow velocity) is a key parameter for flows over obstacles. We evaluate $\hat{h}$ first as a function of lag by averaging the zonal flow and the Brunt–Väisälä frequency over a large volume of inflow depth H upstream of Greenland. The result for $H = 12$ km is displayed in Fig. 7. The mean zonal flow velocity U peaks near $\tau = 0$ for $P = -2$ and has a minimum near $\tau = -0.5$ d for $P = 2$. Clearly, positive torques do not lead to zonal mean flow increases upstream of Greenland. The Brunt–Väisälä frequency exhibits little variation (not shown) near a value of 1.7×10^{-2} s^{-1}, so that the nondimensional mountain height (Fig. 7c) varies $\sim$U^{-1}. In general $\hat{h} \sim 9$ for $h \sim 3000$ m and $P = 0$, but we find even larger values of $\hat{h}$ for $P = 2$ and $-2 \leq \tau \leq 1$ d. The trajectories in Figs. 5 and 6 'feel' at first the mountain height $\hat{h}$ for $\tau = -5$ d but $\hat{h}$ changes with increasing lag for $P \neq 0$. According to Fig. 7, it becomes easier for trajectories to cross Greenland for $P = -2$, while crossing is almost excluded for $P = 2$. This 'prediction' is corroborated in a broad sense by Figs. 5 and 6. Of course, the choice $h \sim 3000$ m is somewhat extreme but a reduction leads simply to a corresponding decrease of $\hat{h}$. A reduction of the inflow depth from 13 to 6 km (Ólafsson and Bougeault, 1997) leads to smaller values of U and thus to even larger ones of $\hat{h}$.

It is well known that the drag $D = (-P - \bar{P})/(a\cos\phi_o)$ exerted by a mountain is proportional to NUh^2 according to linear theories. Ólafsson and Bougeault (1997) point out that the incorporation of surface friction and rotation in numerical experiments constrains the drag to values close to this linear prediction at least for mountains of Pyrenean scale. The results presented by Gill (1982) suggest that the linear drag goes down substantially with increasing half width of the mountain. An interesting 'test' of this relation is provided by Fig. 7a. Indeed, events with strong drag ($P = -2$) exhibit larger zonal flow speeds than those with a rather weak torque ($P = 0$). However, the drag does not grow linearly with U because $Da\cos\phi_o \sim 2$ Hadley for $P = 0$, where $U \sim 5$ m s^{-1} and $\sim$16 Hadley for $P = -2$, where $U = 11$ m s^{-1} at $\tau = 0$. We have to be aware, however, that the drags observed near Greenland and quantified by P are mainly due to synoptic-scale pressure systems. The contribution of

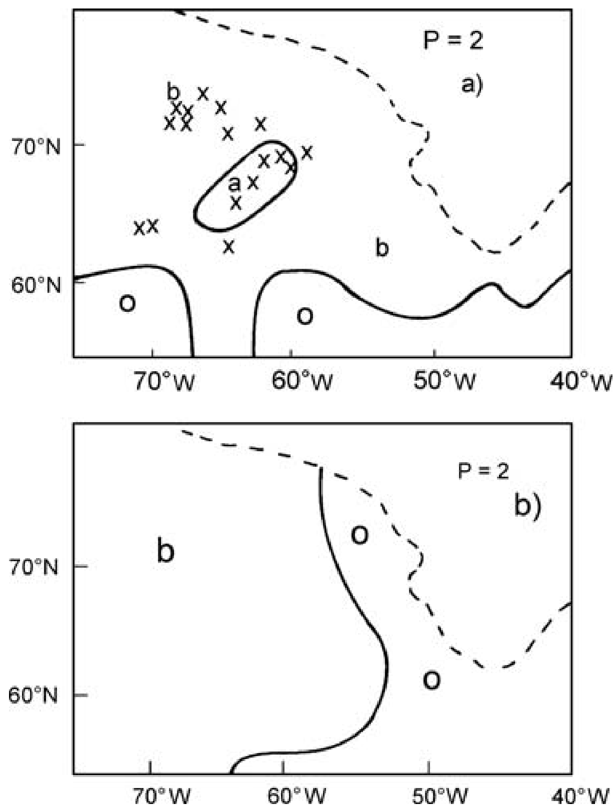

Fig. 6. As Fig. 4 but for $P = 2$.

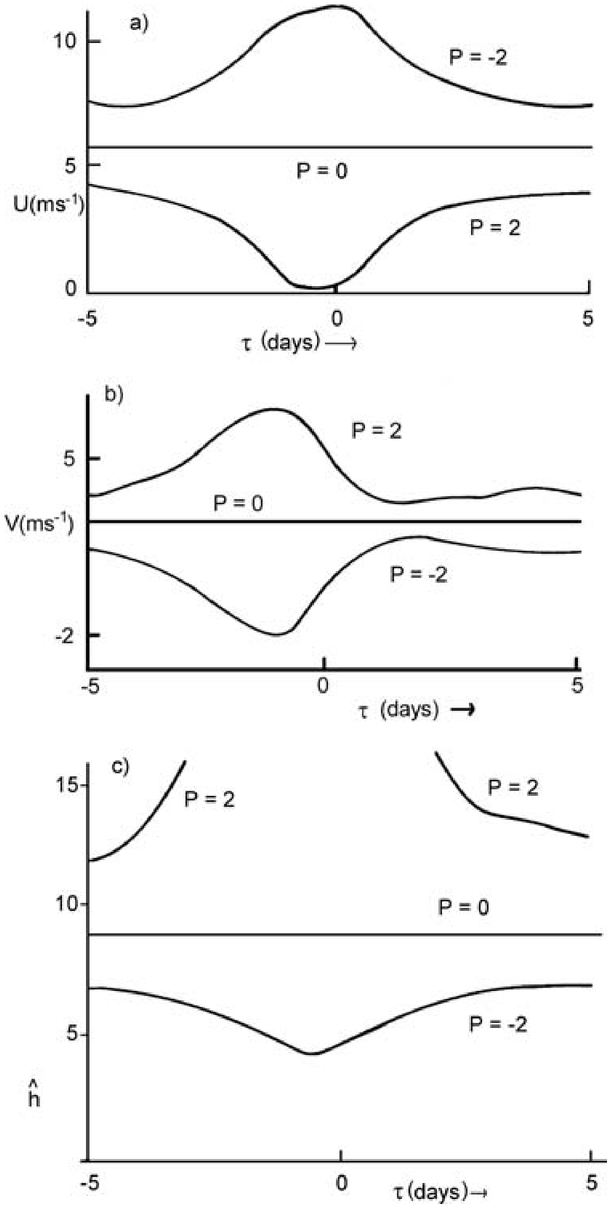

Fig. 7. Mean values (a) U, (b) V in m s^{-1} of the zonal (meridional) wind in a control volume west of Greenland (76°W–59°W; 55°N–72°N; $z \leq 12\,500$ km as a function of lag τ (d) for $P = -2$, 0 and 2. Also given is in (c) the non-dimensional mountain height $\hat{h}$ where an actual height of 3000 m is assumed for Greenland.

quasi-stationary inertia gravity waves as captured, for example, by the linear wave theory in Gill (1982) is presumably small.

As can be seen from the trajectories in Fig. 3, meridional motion is rather important in the inflow region. Fig. 7b demonstrates that the mean meridional velocity V is comparable in magnitude to U. In particular, mean northerlies occur for $P = -2$ near $\tau = 0$. In general however, the flow has a southerly component and in particular, so for $P = 2$. The value of V as an indicator is limited, however, because the mean meridional velocity, say, above Greenland needs not to have the same sign as V as evaluated in the inflow domain.

3.4. Flow splitting

It is clear from Figs. 4–6, that there are many pairs of trajectories which split to attain substantial distances within 10 d. For example, if one trajectory starts in a blocked region close to its boundary and another one in the adjoining domain, say, 'around', there must be complete separation of the two trajectories. This dispersion can be compared to the standard dispersion curve in Fig. 8 where we record the mean distance of pairs of trajectories, started at $z = 500$ m west of Greenland. The longitude of the starting points of a pair is the same and the initial meridional distance is 1.125° (∼100 km). The growth of the distance is slow during the first 5 d. After that, trajectories for $P = -2$ begin to depart faster but the number of pairs declines fairly rapidly in this case because at least one of the partners leaves the domain. The standard deviation of the distances is 520 km for $P = -2$ 580 km for $P = 2$ at $\tau = 0$ while that for $P = 0$ is 514 km.

Flow splitting in the strict sense is a feature of stationary flows and can, therefore not occur in our time dependent circulations except for $P = 0$. On the other hand, strict stationarity is not even found in most numerical simulations so that a certain transience must be accepted. Rapid meridional departure of initially close

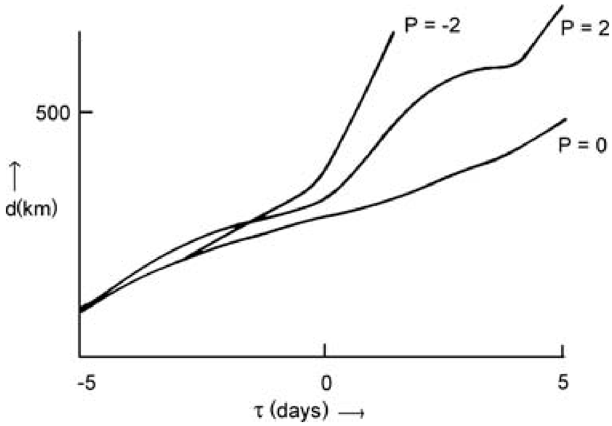

Fig. 8. Mean distance d in 100 km of 483 particle pairs started west of Greenland at $z = 500$ m and at $\tau = -5$ d as a function of lag for the three standard choices of the torque at $\tau = 0$.

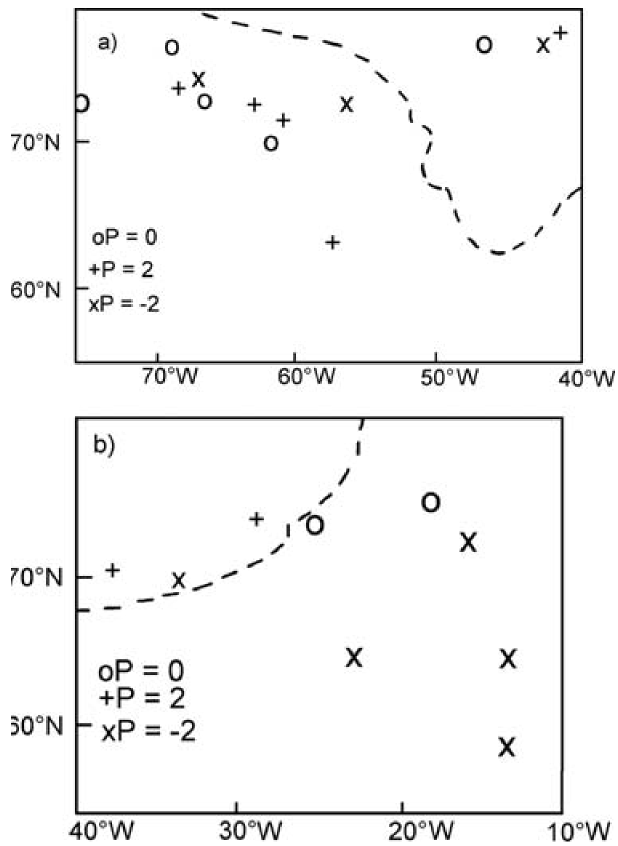

Fig. 9. Stagnation points where trajectories are started at $z = 500$ m. (a) Western part: the stagnation points above Greenland satisfy only a 2 d criterion; (b) eastern part.

trajectories is a sign of flow splitting in any type of flow. Correspondingly, we search for long lasting departures of trajectory pairs due to meridional winds of different sign. More specifically, flow splitting is said to occur if the meridional velocities of a pair are of opposite sign for at least 2 d and if the meridional distance of the trajectories is more than 500 km after that time. This distance is much larger than the mean distance in Fig. 8. The separation of a pair should be less than two grid diagonal distances (~150 km) when the separation begins. Initial points of such splitting events are marked by crosses in Figs. 4a, 5a and 6a where the mean position of a pair is given. It is gratifying that this splitting occurs west of Greenland for $P = 0$ partly in the blocked region and partly in the region where 'over-trajectories' start. It is somewhat surprising that this type of splitting occurs less often for $|P| = 2$ than for $P = 0$, but the criterion that the sign of the meridional velocities of a pair has to differ for 2 d is fairly strict and easier to satisfy for stationary flow. Flow splitting is found more frequently again in the blocked area for $P = 2$ (see Fig. 6a), if trajectories start at $\tau = -3$ d (not shown).

It may come as a surprise that splitting is so common for $P = 0$. The winds in Fig. 1 are fairly uniform and it is hard to find any place where flow splitting might occur. We have to bear in mind, however, that the climatic mean flow at the next level west of Greenland has a southerly component. Thus, if the vertical velocity of a pair differs, one partner may stick to the northerlies while the other one is caught in the southerly regime.

The flow splitting diagnosis as presented is somewhat biased because pairs may leave the domain before the 2 d criterion is satisfied. This effect restricts presumably the number of splitting events near the tip.

3.5. Stagnation points

Flow stagnation is also a transient phenomenon in our data. We adopt the criterion that a trajectory is called stagnant if the 'particle' moves less than 5 km in 16 consecutive 6 hr intervals, that is, the trajectory stays almost at the same place for at least 4 d. Some of these stagnation points are shown in Fig. 9. In fact, more such points are found in the data but they cluster near those shown. Stagnation west of Greenland (Fig. 9a) occurs for all values of P and prefers the northwestern part of our domain. That is, of course, also the area where blocked flows are common. The events in Fig. 9a are observed for trajectories starting at $z = 500$ m. Stagnation in numerical experiments tends to occur at the windward slope and at points above the leeward slope (Smith and Grønås, 1993). The stagnation points in Fig. 9a are not located above the slopes of Greenland. There are some above the crest of Greenland. Stagnation is also observed for starting points at $z = 1500$ m, but not for departure points higher up. Stagnation occurs above the lee slope (Fig. 9b) and also off Greenland at least for $P = -2$ where anticyclonic circulations prevail. Stagnation is found in the east also for trajectories starting at 2500 m (not shown). It has to be stressed again that we are looking here at statistical trajectories where stagnation implies little mean motion for a given torque and lag. It is open, if actual trajectories stagnate for such long times.

3.6. Tip jet

We expect to find strong westerlies near the tip of Greenland for $P = -2$ where low pressure is found east of Greenland. For example, the torque in the case selected by Doyle and Shapiro (1999) is obviously negative. To find out about tip jets in our climatology we simply have to search for strong westerlies at the lowest level east of Greenland. If we prescribe a threshold of 13 ms^{-1}, we find that jets occur indeed in the area southeast of the tip marked by dots in Fig. 1 if $P = -2$. There are no jets for $P = 0$ and, of course, none for $P = 2$. Moreover, the tip jet is found only for $\tau = 0$ even if $P = -2$.

It is tempting to interpret the lee side low found to the north of the tip jet as the wake vortex found in numerical simulations for relatively high values of $\hat{h}$. We have to bear in mind, however, that these lows are highly transient and form under specific synoptic conditions. Moreover, there is a corresponding high for $P = 2$. Leeside highs are not found in numerical simulations.

4. Discussion and conclusion

In this paper, a novel technique has been applied to flow observations near Greenland in order to explore flow characteristics with respect to this obstacle for various synoptic situations. The axial mountain torque exerted by Greenland has been selected as a parameter which characterizes the basic surface pressure distribution in the Greenland area. High pressure prevails in the lee of the massif and low pressure near the tip for $P > 0$. It is the opposite for $P < 0$. The statistical trajectories as calculated from the wind field statistics according to (2) vary quite strongly with the torques. This allows us to study the blocking characteristics of Greenland with respect to the torque and also with respect to the related basic synoptic situations. This approach is elegant and self-consistent but has the obvious drawback that the trajectories based on (2) have not been observed but represent likely flow paths. It is desirable to complement this work with investigations of trajectories derived with standard methods as presented, for example, by Schwierz (2001) in a Greenland case study. Although it is not possible to construct the covariances of trajectories with respect to the torque, one could, for example, look at trajectories starting, say, 5 d before selected days with large positive torques. This strategy would give bundles of trajectories to be evaluated statistically. It is expected that our statistical scheme anticipates the main results of this future effort. These expectations are constrained by the fact that the evaluation of the statistical trajectories in this paper is relatively crude at least near the ground where the vertical resolution of the grid is 1000 m. It must be stressed that cases with $|P| = 2$ represent relatively rare and strong torque events.

It has been found that flow blocking is particularly strong for positive torques in rough agreement with the evaluation of non-dimensional heights. The small values of the mean zonal flow U are reflected in large values of $\hat{h}$ for $P = 2$. Blocking is not so common for $P = -2$ when most trajectories go around Greenland. There are, however, always many starting points for trajectories crossing Greenland. Tip jets are found for $P = -2$ and $\tau \sim 0$ only. Stagnation as well as flow splitting is common west of Greenland and occurs even in the absence of torques. Stagnation is also found above Greenland's crest and above the eastern slope. We have to stress again that this is statistical stagnation. It is unlikely, but conceivable that stagnation never occurs east of Greenland despite our findings. That would happen, in particular, if the torque were an inefficient parameter. Actual flows would be unrelated to P in that case and the flow covariances $C(P, \mathbf{v}|\tau)$ would be quite small in contrast to what is found. Nevertheless, it is conceivable that there are, say, events of tip jets or flow splitting which are not accompagnied by torque events. These are missed by our approach. That is, however, not a shortcoming of the method. After all, the data are stratified with respect to the torque. We wish to study the flows typical of torque events. Other situations are beyond the scope of this paper.

References

Doyle, J. and Shapiro, M. 1999. Flow response to large-scale topography: the Greenland tip jet. *Tellus* **51A**, 728–748.

Doyle, J., Shapiro, M., Jiang, Q. and Bartels, D. 2005. Large-amplitude mountain wave breaking over Greenland. *J. Atmos. Sci.* **62**, 3106–3126.

Egger, J. 1972. Incorporation of steep mountains into numerical forecasting models. *Tellus* **24**, 324–335.

Egger, J. and Hoinka, K.-P. 2006. Dynamics of atmospheric regression patterns: regional mountain torque events. *J. Atmos. Sci.* **63**, 1467–1482.

Gill, A. 1982. *Atmosphere-Ocean Dynamics*. Int. Geophys. Ser. 30, Ac. Press. 622 pp.

Hoskins, B. and Hodges, K. 2002. New perspectives on the northern hemisphere winter storm tracks. *J. Atmos. Sci.* **59**, 1041–1061.

Iskenderian, H. and Salstein, D. 1998. Regional sources of mountain torque variability and high-frequency fluctuations in atmospheric angular momentum. *Mon. Weather Rev.* **128**, 1681–1694.

Moore, G. and Renfrew, I. 2005. Tip jets and barrier winds: a Quick SCAT climatology of high wind speed events around Greenland. *J. Climate* **18**, 3713–3725.

Ólafsson, H. and Bougeault, Ph. 1996. Nonlinear flow past an elliptic mountain. *J. Atmos. Sci.* **53**, 2465–2489.

Ólafsson, H. and Bougeault, Ph. 1997. The effects of rotation and surface friction on orographic drag. *J. Atmos. Sci.* **54**, 193–210.

Petersen, G., ?lafsson H. and Kristjánsson, J. 2003. Flow in the lee of idealized mountains and Greenland. *J. Atmos. Sci.* **60**, 2183–2195.

Putnins, P. 1970. The climate of Greenland. World Survey of Climatology. In: Vol. 14, *Climates of the polar regions* (ed S. Orrig). Elsevier, Amsterdam, pp. 1–128.

Schär, Ch. and Smith, R. 1993. Shallow water flow past isolated topography. Part I: vorticity production and wake formation. *J. Atmos. Sci.* **50**, 1373–1400.

Schwierz, C. 2001. *Interaction of Greenland-Scale Orography and Extra-Tropical Synoptic-Scale-Flow*. Diss. ETH Zürich, 155 pp.

Schwierz, C. and Davies, H. 2003. Evolution of a synoptic-scale vortex advecting toward a high mountain. *Tellus* **55A**, 158–172.

Smith, R. and Grønås, S. 1993. Stagnation points and bifurcation in 3-D mountain airflow. *Tellus* **45A**, 606–623.

Uppala, S. and co-authors. 2006. The ERA re-analysis. *Q. J. R. Met. Soc.* **131**, 2961–3012.

Walden, H. 1959. *Statische-synoptische Untersuchungen über das Verhalten von Tiefdruckgebieten im Bereich von Grönland (Statistic-synoptic investigations on cyclones near Greenland)*. Deutsch. Wetterdienst. Seewetteramt. Einzelveröffentlichung 20, pp. 70.

Weickmann, K. 2003. Mountains, the global friction torque and the circulation over the Pacific North American region. *Mon. Weather Rev.* **131**, 2608–2622.